

3.5 W Broadband PM Hybrid Amplifier at 2051 nm with Holmium- and Thulium-Doped Single-Clad Fibers

Robert E. Tench, *Senior Member, IEEE*, Alexandre Amavigan, Clement Romano, Daniya Traore, Jean-Marc Delavaux, *Senior Member, IEEE*, Thierry Robin, Benoit Cadier, Arnaud Laurent, and Patrice Crochet

Abstract— We report the design and performance of a packaged broadband PM hybrid HDFA/TDFA in the 2000–2100 nm band using all-single-clad doped fibers. Internal small signal $G = 49.1$ dB, small signal NF = 6.5 dB, and $P_{out} = 3.54$ W are achieved at $\lambda_s = 2051$ nm. The simulated 3 dB output power bandwidth is 98 nm. Comparisons of experimental data and simulations show good agreement. We investigate through simulations an all-Holmium two stage PM optical amplifier design for comparison to the hybrid PM HDFA/TDFA.

Index Terms— Doped Fiber Amplifiers, Infrared Fiber Optics, Optical Fiber Devices, Holmium, Thulium, Polarization Maintaining Fiber, 2 microns.

I. INTRODUCTION

The rapid development of polarization maintaining (PM) Ho- and Tm-doped optical fiber amplifiers in the 2000 nm spectral region is important for many emerging applications including LIDAR, optical telecommunications, and spectral sensing [1]–[7]. In previous work, it has been shown that hybrid PM Holmium-doped fiber amplifier (HDFA) and Thulium-doped fiber amplifier (TDFA) architectures using single-clad and double-clad fibers exhibit low noise figure (NF), high output powers, and a large operating spectral bandwidth [8]–[15]. However, the use of double clad Tm-doped fibers requires a temperature stabilized 793 nm pump source, which is not an optimum choice for compact high performance packaged optical amplifier modules.

In this paper, we propose and demonstrate a hybrid PM HDFA/TDFA using all single-clad doped fibers. Our new

architecture is capable of high optical output powers, exhibits a wide operating bandwidth and low NF, and additionally operates with an uncooled 940 nm semiconductor pump laser source, leading to a high performance compact packaged amplifier module for the 2000–2100 nm spectral region. We also compare the performance of our hybrid design to an all-Holmium two stage fiber amplifier with comparable fiber pump powers.

The structure of our paper is as follows: The experimental setup and architecture for our hybrid PM HDFA/TDFA is given in Section II. Here we include a description of a compact packaged and integrated realization of our amplifier design. Section III contains experimental and initial simulated results for the performance of the broadband high gain full hybrid amplifier. In Section IV, we compare the results from our hybrid amplifier to the simulated performance of an optimized all-Holmium two stage design. Finally, Section V discusses the results of our investigations and compares our new amplifier designs to previous results from the literature.

II. EXPERIMENTAL SETUP, PACKAGING, AND INTEGRATION

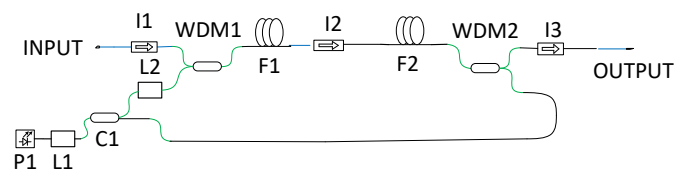


Fig. 1. Optical schematic of hybrid PM HDFA/TDFA

A schematic diagram of the hybrid PM HDFA/TDFA is shown in Fig. 1. Signal input light at 2000–2100 nm passes through isolator I1 and 1940/2050 nm WDM1 and is coupled into F1, a 3.0-m-long PM Ho-doped fiber (iXblue IXF-HDF-PM-8-125). The signal output from F1 is coupled through isolator I2 into F2, a 2.5-m-long PM Tm-doped fiber (iXblue IXF-TDF-PM-5-125). The amplified output of F2 passes through WDM2 and I3 to the signal output port. Internal input signal power P_s is measured at the input of F1, and internal signal output powers are measured at the outputs of F1 and F2. In this amplifier, P1 is a multiwatt 940 nm semiconductor laser diode which pumps L1, a 1560 nm multiwatt Er-Yb fiber laser. Coupler C1 splits the output of L1 in a 50/50 ratio, and

Manuscript submitted on October 16, 2020.

Robert E. Tench, Alexandre Amavigan, and Jean-Marc Delavaux are with Cybel LLC, 1195 Pennsylvania Avenue, Bethlehem, PA 18018 USA (e-mail: robert.tench@cybel-llc.com) (alexandre.amavigan@cybel-llc.com) (jm@cybel-llc.com).

Clement Romano is with Fraunhofer IOSB, Gutleuthausstraße 1, 76275 Ettlingen, Germany (e-mail: clement.romano@iosb.fraunhofer.de)

Daniya Traore is with École Nationale Supérieure des Sciences Appliquées et de Technologie, Lannion, France (e-mail: daniya-traore@outlook.fr)

Thierry Robin, Benoit Cadier, Arnaud Laurent, and Patrice Crochet are with iXblue Photonics, Lannion, France (e-mail: thierry.robin@ixblue.com) (benoit.cadier@ixblue.com) (arnaud.laurent@ixblue.com) (patrice.crochet@ixblue.com)

50% of the output of L1 is used as an input to L2, a 1940 nm multiwatt Tm-doped fiber laser which then copumps F1 through WDM1. The other 50% of the 1560 nm output of L1 counterpumps F2 through WDM2. Up to 2.5 W of 1940 nm pump light is available to pump F1, and up to 5 W of 1560 nm pump light is available to pump F2.

The fully packaged and integrated amplifier incorporates electronic control circuits for the pump laser and for monitoring the signal input power. Communication with the amplifier is via RS232 and USB interfaces. The mass is 600 g. Electrical power consumption for the packaged device is 66 W at full optical output power. Fig. 2 is a photograph of the packaged amplifier.



Fig. 2. Packaged hybrid HDFA/TDFA ($200 \times 150 \times 43 \text{ mm}^3$).

III. EXPERIMENTAL AND SIMULATED RESULTS

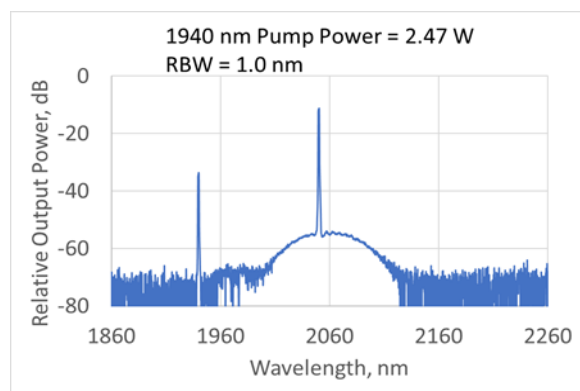


Fig. 3. : Mid-stage output spectrum for the hybrid PM HDFA/TDFA

Fig. 3 shows the mid-stage output spectrum of the preamplifier (at the output of F1) for $P_s = -1.6 \text{ dBm}$ @ 2051 nm. The 1940 nm pump power for this spectrum is 2.5 W. Here we measure an internal peak signal power of 580 mW. The pump feedthrough at 1940 nm is 23 dB down from the peak signal indicating efficient use of the pump power in the first amplifying stage.

In Fig. 4 we plot the output spectrum of the full amplifier with 1560 nm pump power of 5 W in F2 and 1940 nm pump power of 2.5 W in F1. Here the measured internal signal power at the output of F2 is 3.54 W. It is interesting to note that the 1940 nm pump feedthrough is now only 14 dB down from the peak of the signal, indicating that the Tm-doped second stage is amplifying the pump feedthrough from the first stage. From the -10 dB width of the ASE below the signal

peak we estimate the 3 dB output power bandwidth of the full amplifier to be 95 nm (2000–2095 nm).

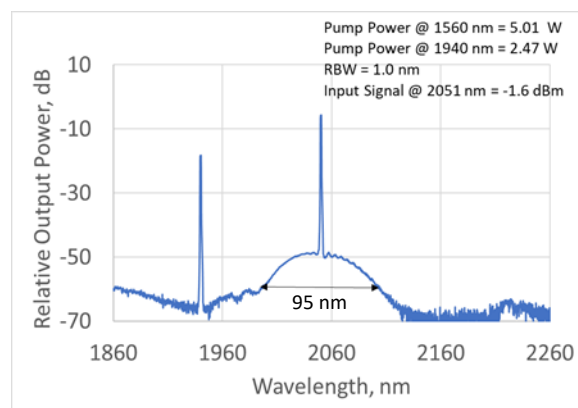


Fig. 4. Output spectrum of the full hybrid HDFA/TDFA

Fig. 5 shows the measured internal signal power at the output of F2 as a function of the power delivered from the 940 nm semiconductor pump laser. The maximum amplified 2051 nm signal power at 33.7 W pump power is 3.54 W. We observe that the variation of output power with pump power follows a linear trend above 9 W with a slope of 13.4%.

The long term stability of the output power of the hybrid packaged HDFA/TDFA is measured to be 1% p-p over a period of 3 hours. The polarization extinction ratio at the output of the amplifier is determined by I3 and is $> 20 \text{ dB}$.

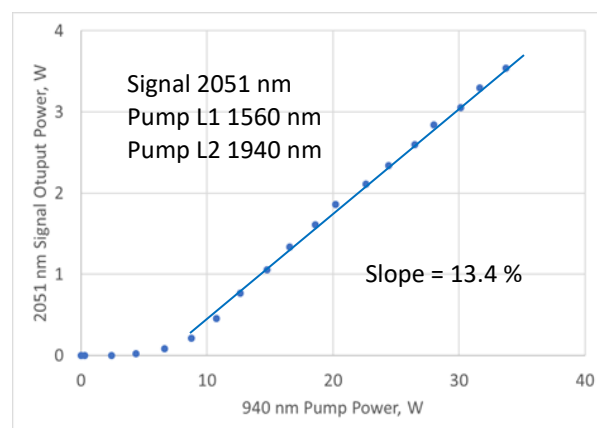


Fig. 5. Measured internal P_{out} at 2051 nm vs. 940 nm pump laser power for $P_s = -1.6 \text{ dBm}$

We have also simulated the performance of our hybrid PM HDFA/TDFA using the techniques developed and reported previously [15]. Fig. 6 shows the experimental and simulated internal gain (G) and NF for the packaged amplifier as a function of 2051 nm input signal power P_s . Here the points are data and the lines are simulations. The maximum small signal gain at this wavelength is measured to be 49.1 dB, and the simulated gain is 51.5 dB which agrees relatively well with the data. The minimum experimental small signal NF is 6.45 dB, and the simulated value is 7.23 dB, indicating good agreement. This high G and low NF indicate that the hybrid amplifier will be useful as a preamplifier for lightwave

communication systems, and also as an amplifier for pulsed input signals with low duty cycles. The evolution of G and NF with P_s shows a good match between experiment and simulation and follows the expected trend for a high gain fiber optical amplifier. The input signal dynamic range for $G > 35$ dB is 37.4 dB.

The simulated value of output power for the HDFA preamplifier with $P_s = -1.6$ dBm @ 2051 nm is 563 mW and this value is in excellent agreement with the measured power of 580 mW in Fig. 3.

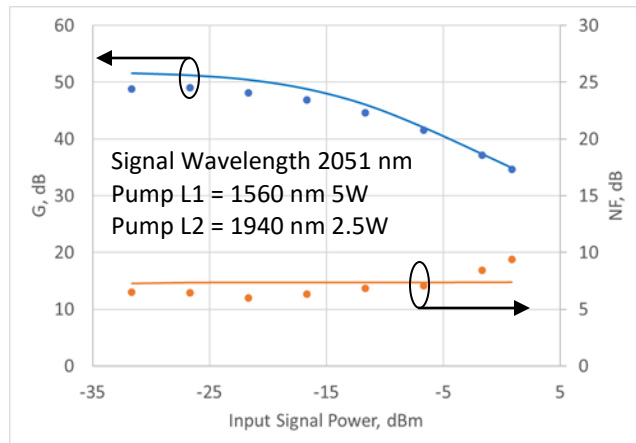


Fig. 6. Measured and simulated internal gain G and NF at 2051 nm as a function of P_s .

In Fig. 7, we present the evolution of G and NF as a function of signal wavelength from 1990–2110 nm. Here, the 1560 nm pump power was 5 W and the 1940 nm pump power was 2.5 W. The points are simulated values and the lines are polynomial fits to the simulations. From this plot, we note that the maximum internal small signal gain expected from this amplifier is 53.2 dB at a wavelength of 2030 nm. The simulations indicate that an amplifier gain of greater than 35 dB is expected for a wavelength range of 1988–2098 nm or 110 nm, indicating wide bandwidth gain operation of the amplifier.

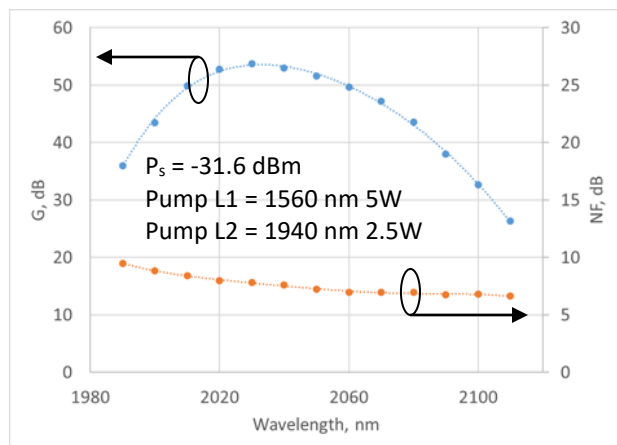


Fig. 7. Simulated internal G and NF vs. signal wavelength

In Fig. 8, we have plotted the simulated and experimental values of internal output power for $P_s = -1.6$ dBm, 1560 nm pump power of 5 W, and 1940 nm pump power of 2.5 W. Here, the experimental data are points and the dashed line is a polynomial fit to the simulations. We see that the 3 dB (50%) output power width of the simulated curve is 1992–2090 nm or 98 nm, which agrees quite well with the estimated value of 95 nm derived from Fig. 3. However the experimental curve has a 3 dB width of about 88 nm primarily due to the measured dropoff in measured output power at 2004 nm. The reasons for the discrepancy at 2004 nm are under active investigation, and may include inaccuracies in cross sectional data and spectral losses with wavelength in the passive components. The maximum simulated output power at 2051 nm is 3.71 W, which agrees well with the value of 3.54 W that is measured in Figs. 4 and 5.

We note that the fiber lengths chosen for the Ho- and Tm-doped fibers in the amplifier are optimized for a signal wavelength of 2051 nm. By selecting significantly longer fiber lengths we expect to extend the spectral response of the amplifier to wavelengths greater than 2100 nm [15]. We also expect the maximum output power to scale linearly with available pump power, and an output signal power of 10 W should therefore be possible.

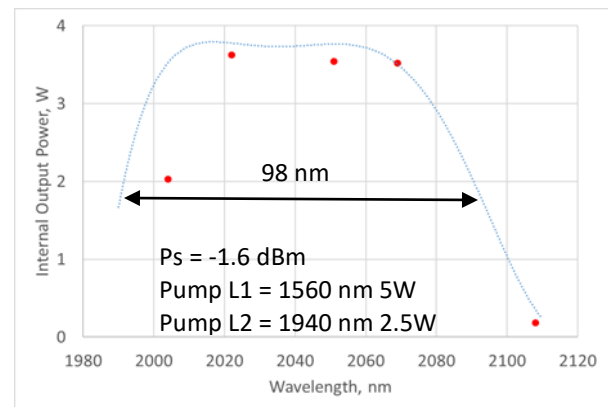


Fig. 8. Simulated (dashed line) and experimental (points) internal output power vs. wavelength

We observe that in our amplifier, the insertion losses of the PM optical isolators are about 1.2 dB and the signal channel insertion losses of the PM WDMs are about 0.4 dB. The input signal coupling loss is then found to be 1.7 dB (including fiber splice losses), the interstage coupling loss is 1.4 dB, and the output signal coupling loss is 1.7 dB. Therefore, the packaged or fiber to fiber gains are 3.4 dB smaller than the internal G values, and the packaged or fiber to fiber output powers are 1.7 dB smaller than the quoted internal output powers.

IV. COMPARISON WITH THE PERFORMANCE OF AN OPTIMIZED TWO-STAGE ALL-HOLMIUM DESIGN

To contrast the behavior of our hybrid HDFA/TDFA with a comparable all Ho-doped amplifier design, we consider the optical amplifier architecture shown below in Fig. 9. Here F1

and F2 are Ho-doped PM fibers identical to the fiber in Fig.1 (IXF-HDF-PM-8-125). P1 is a 40 W rated 940 nm multimode semiconductor laser diode that pumps L1, a 1560 nm ErYb-doped fiber laser with 10 W maximum output power as before. (As in the hybrid amplifier, the power conversion efficiency of L1 is $\sim 25\%$). L1 then pumps L2, a 1940 nm Tm-doped fiber laser with 5 W maximum output power. (As in the hybrid amplifier, the power conversion efficiency of L2 is $\sim 50\%$). In the same manner as the amplifier in Fig. 1, a pump wavelength of 1940 nm was chosen based on a survey of the existing literature [16]–[22] and the gain and absorption curves for the Ho-doped fiber [8],[20]. Coupler C1 splits the 1940 nm output of L1 between preamplifier stage F1 and power amplifier stage F2. Wavelength division multiplexers WDM1 and WDM2 are employed to co-pump both Ho-doped amplifier stages, and isolators I1–I3 prevent external feedback and the buildup of ASE from affecting the performance of the amplifier.

To find the optimum split ratio for C1 and the optimum fiber lengths for F1 and F2, we carried out a multiparameter simulation of amplifier performance with the objective of reaching maximum amplified output power at a signal wavelength of $\lambda_s = 2050$ nm and a saturating input signal power of $P_s = -1.6$ dBm. The results of this optimization yielded the following values for the total available 1940 nm pump power of 5 W: C1 = 30% to the preamp, 70% to the power amp; F1 = 3.0 m; and F2 = 2.0 m. We use these values in all of our two stage Ho-doped amplifier simulations going forward.

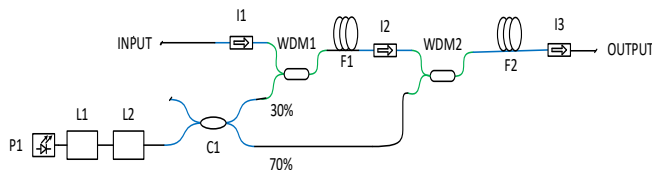


Fig. 9. Optical schematic of all Ho-doped fiber amplifier design for comparison to the hybrid HDFA/TDFA in Fig. 1.

We begin our simulation studies by plotting the small signal gain and noise figure as a function of input signal power for the all Ho-amplifier. Fig. 10 shows the results of these simulations, where the maximum small signal gain reaches the high value of 60 dB at the minimum input signal power of $P_s = -31.5$ dBm. In comparison to the hybrid amplifier in Fig. 6, the all-Ho amplifier exhibits 8.5 dB greater small signal gain. The noise figures for the two amplifiers are the same at 7.4 dB.

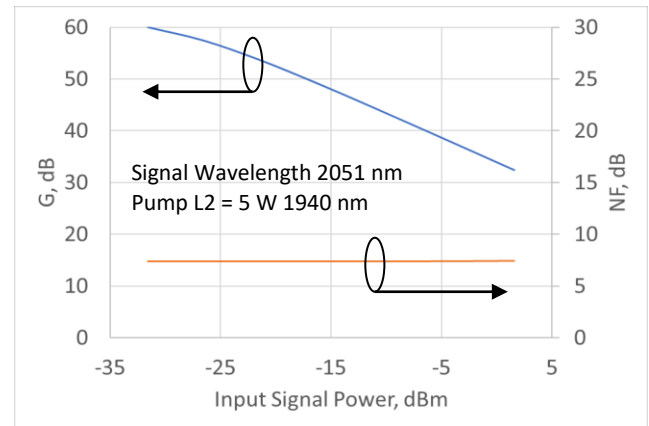


Fig. 10. Simulated G and NF as a function of P_s for the all-Ho amplifier design

Our next simulation study, for small signal gain and noise figure as a function of signal wavelength, is presented in Fig. 11. Here we see the 25 dB gain bandwidth of the small signal gain is from 1988–2180 nm or 120 nm. This broad region of high gain operation is important for preamplifier applications in WDM lightwave systems. When we compare these results to the performance of the hybrid HDFA/TDFA in Fig. 7, we find that the hybrid amplifier exhibits the same 25 dB gain bandwidth of 120 nm. The noise figures as a function of signal wavelength behave similarly for the two amplifier designs.

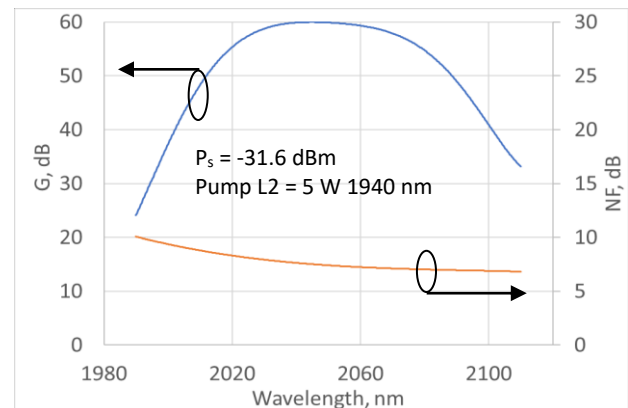


Fig. 11. Simulated G and NF as a function of λ_s for the all-Ho amplifier design.

Finally in Fig. 12 we plot the simulated saturated output power of the all-Ho amplifier as a function of signal wavelength. From this plot, we see that the maximum saturated output power at 2050 nm is 2.44 W. This value is significantly less than the 3.84 W that is obtained with the hybrid amplifier in Fig. 8, and the reduction represents a factor of 2.0 dB in output power. However the 3 dB output power bandwidth of 98 nm is the same as the value for the hybrid amplifier in Fig. 8.

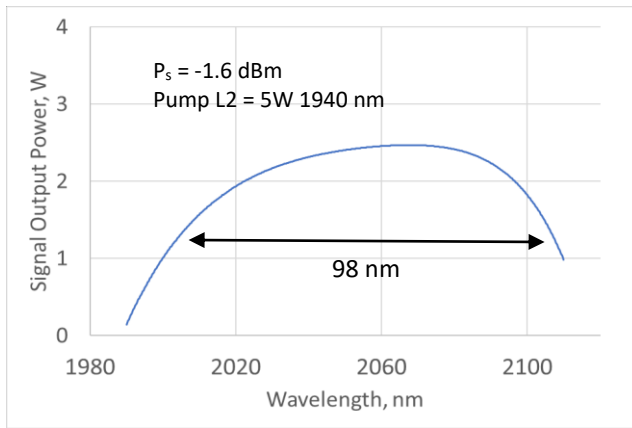


Fig. 12. Simulated saturated output power as a function of λ_s for the all-Ho amplifier design

The important internal performance characteristics of the two amplifier designs are summarized in Table 1.

Parameter	Hybrid HDFA/TDFA	All-Ho Design
Maximum G	51.5 dB	60 dB
25 dB Gain BW	120 nm	120 nm
Output Power BW	98 nm	98 nm
Maximum P _{out}	3.84 W	2.44 W

Table 1. Comparison of hybrid HDFA/TDFA and all Ho-fiber amplifier simulated performance

V. DISCUSSION

In all our amplifier measurements, the linearly polarized signal light in the 2 μm band propagates through the fibers on the slow axis. This choice was made to be consistent with standard industry practices for PM amplifiers. We note that the pump signals at 1560 nm and at 1940 nm in our hybrid PM HDFA/TDFA are not polarization controlled. This contrasts with the results in [9] where the pump light at 1940 nm was linearly polarized in the HDFA preamp. Future studies will cover the case of linearly polarized pump signals at 1560 nm and 1940 nm.

In our studies of simulation and experiment for amplifier gain G and noise figure NF with a 1940 nm HDFA pump, we observe that agreement between simulations and data for the full hybrid PM HDFA/TDFA amplifier is good. We observe that the following factors may influence the accuracy of our simulations for noise figure and gain:

1) Our gain and absorption curves for the Ho-doped fiber and the Tm-doped fiber are derived both from measurements by the manufacturer iXblue and from the literature [8],[20].

We observe that composition may play a large role in the performance of the fibers, While the shapes of the cross sections are expected to be similar to the fibers in this paper, there may still be significant variations in the fiber compositions.

Future studies will be carried out to directly measure the gain and absorption curves for these fibers, to remove potential sources of uncertainty in the absorption and emission

data which are currently estimated from reports in the literature and initial measurements from the manufacturer.

2) Our measurement of NF is carried out without a narrow bandpass filter between the semiconductor laser source and the input port of the fiber amplifier. The function of this bandpass filter is to remove the spontaneous emission background of the laser source. Future experimental studies will incorporate a narrow bandwidth optical filter to remove effects of the background of the laser source on measurements of NF for high input signal powers [23].

One possible source of excess noise is the introduction of long wavelength ASE from the high power Tm-doped pump laser into the Ho-doped fiber through imperfections in the 1940/2050 nm WDM. This would present as additional noise in the 2000–2100 nm signal range of the amplifier. The possibility of excess noise introduced by this mechanism will be investigated in the future.

No stimulated scattering processes, such as SBS and SRS, are seen during our measurements, as indicated by the fully linear experimental behavior of P_{out} vs. P_{pump} . (Significant backwards Brillouin scattering would cause a significant sublinear variation in P_{out} vs. P_{pump} and no such behavior is seen.)

The simulated operating bandwidth of 98 nm for the hybrid single clad HDFA/TDFA agrees well with the value of ≥ 90 nm for the double clad HDFA/TDFA reported in [15]. To our knowledge, this is the first direct observation of the operating bandwidth of a hybrid single clad HDFA/TDFA design. Such a wide operating bandwidth is highly advantageous in a variety of applications, particularly for LIDAR and spectral sensing.

Following studies of the hybrid amplifier design, we introduced a comparable two stage all-Ho architecture with equivalent pump powers. Our simulations study of the all-Ho amplifier indicates that this design delivers significantly higher small signal gain (by 8.5 dB), significantly lower saturated output power (by 2.0 dB), and equivalent small signal gain bandwidths and output power operating bandwidths in comparison to the hybrid HDFA/TDFA.

We note that the significantly higher output power obtained from the hybrid design is quite advantageous in applications such as spectral sensing and LIDAR.

Future work will concentrate on two areas:

1) Experimental verification of the simulation results for the two-stage HDFA amplifier design, and

2) Further extending the bandwidth of the hybrid amplifier to longer signal wavelengths in the region of 2100-2130 nm by modifying the pumping wavelengths of the Ho-doped and Tm-doped fibers, by changing the material composition of the fibers, and by adjusting the fiber lengths [15].

VI. SUMMARY AND CONCLUSIONS

We have presented a novel packaged hybrid polarization maintaining 2000 nm band HDFA/TDFA design employing all single-clad fibers and an uncooled 940 nm semiconductor pump laser. The dimensions of the packaged amplifier are 200

$\times 150 \times 43 \text{ mm}^3$, the maximum experimental internal output power achieved at 2051 nm is a high value of 3.54 W, the internal small signal gain at this signal wavelength is 49.1 dB, and the internal small signal noise figure is 6.5 dB. The wide 3 dB output power bandwidth of the hybrid HDFA/TDFA is estimated to be 88–98 nm (from 1992–2090 nm) both from our data and simulation results. There is good agreement between our experimental measurements and simulations that we plan to explore further.

Our simulation studies of a comparable all-Ho amplifier design indicate that the hybrid HDFA/TDFA design yields significantly higher saturated output power, significantly lower small signal gain, and equivalent gain bandwidth and output power operating bandwidth. Selection of one or the other of these two designs will depend on the specific details of the applications for the amplifiers.

Potential applications of our packaged hybrid PM HDFA/TDFA include space, avionics, LIDAR, WDM telecommunications, and spectral sensing.

VII. FUNDING

This work was funded by the United States government through NASA SBIR Phase 1 Contract # 80NSSC19C0278.

VIII. REFERENCES

- [1] G. D. Spiers et al., "Atmospheric CO₂ measurements with a 2 μm airborne laser absorption spectrometer employing coherent detection," *Applied Optics* 50, 2098-2111 (2011).
- [2] J. Caron and Y. Durand, "Operating wavelengths optimization for a spaceborne lidar measuring atmospheric CO₂," *Applied Optics* 48, 5413–5422 (2009).
- [3] J. B. Abshire, H. Riris, G. R. Allan, C. J. Weaver, J. Mao, X. Sun, W. E. Hasselbrack, and A. Yu, A. Amediak, Y. Choi, and E. V. Browell, "A lidar approach to measure CO₂ concentrations from space for the ASCENDS mission," *Proc. SPIE* 7832, 783201 (2010).
- [4] M. U. Sadiq et al., "40 Gb/s WDM Transmission Over 1.15-km HC-PBGF Using an InP-Based Mach-Zehnder Modulator at 2 μm ," *J. Lightwave Technology* 34, 1706-1711 (2016).
- [5] H. Zhang et al., "Dense WDM Transmission at 2 μm Enabled by an Arrayed Waveguide Grating," *Optics Letters* 40, 3308-3311 (2015).
- [6] H. Zhang et al., "100 Gbit/s WDM Transmission at 2 μm : Transmission Studies in Both Low-loss Hollow Core Photonic Bandgap Fiber and Solid Core Fiber," *Optics Express* 23, 4946-4951 (2015).
- [7] H. Zhang et al., "81 Gb/s WDM Transmission at 2 μm over 1.15 km of Low-Loss Hollow Core Photonics Bandgap Fiber," in *Proc. ECOC 2014*, Cannes, France, paper P.5.20.
- [8] R. E. Tench, C. Romano, and J.-M. Delavaux, "A 25 W 2 μm Broadband Polarization-Maintaining Hybrid Ho- and Tm-Doped Fiber Amplifier," *Applied Optics* 58, 4170-4175 (2019).
- [9] Robert E. Tench, Clement Romano, and J.-M. Delavaux, "Studies of the Optical Bandwidth of a 25 W 2 μm Band PM Hybrid Ho-/Tm-Doped Fiber Amplifier", in *Proc. SPIE 11000*, Fiber Optic Sensors and Applications XVI, Defense and Commercial Sensing, Baltimore, MD, Paper 11000-8 (April 2019).
- [10] R. E. Tench, C. Romano, J.-M. Delavaux, T. Robin, B. Cadier, and A. Laurent, "Broadband High Gain Polarization-Maintaining Holmium-Doped Fiber Amplifiers," in *Proc. ECOC 2018*, Rome, Italy, September 2018, Paper Mo3E.3.
- [11] Robert E. Tench, Clement Romano, Glen M. Williams, Jean-Marc Delavaux, Thierry Robin, Benoit Cadier, and Arnaud Laurent, "Two-Stage Performance of Polarization-Maintaining Holmium-Doped Fiber Amplifiers," *IEEE Journal of Lightwave Technology* 37, 1434–1439 (2019).
- [12] Z. Li, A. M. Heidt, J. M. O. Daniel, Y. Jung, S. U. Alam, and D. J. Richardson, "Thulium-doped fiber amplifier for optical communications at 2 μm ," *Opt. Express* 21, 9289-9297 (2013).
- [13] Z. Li, A. M. Heidt, N. Simakov, Y. Jung, J. M. O. Daniel, S. U. Alam, and D. J. Richardson, "Diode-pumped wideband thulium-doped fiber amplifiers for optical communications in the 1800 – 2050 nm window," *Opt. Express* 21, 26450-26455 (2013).
- [14] Robert E. Tench, Clement Romano, and Jean-Marc Delavaux, "Shared Pump Two-Stage Polarization-Maintaining Holmium-Doped Fiber Amplifier," *IEEE Photonics Technology Letters* 31, 357–360 (2019).
- [15] R. E. Tench et al., "In-Depth Studies of the Spectral Bandwidth of a 25 W 2 μm Band PM Hybrid Ho- and Tm-Doped Fiber Amplifier", *J. Lightwave Technol.*, vol 38, pp. 2456–2463 (2020).
- [16] A. Hemming, N. Simakov, A. Davidson, M. Oermann, L. Corena, D. Stepanov, N. Carmody, J. Haub, R. Swain, and A. Carter, "Development of high-power Holmium-doped fibre amplifiers," *Proc. SPIE 8961*, Fiber Lasers XI: Technology, Systems and Applications, 89611A (7 March 2014).
- [17] N. Simakov, Z. Li, Y. Jung, J. M. O. Daniel, P. Barua, P. C. Shardlow, S. Liang, J. K. Sahu, A. Hemming, W. A. Clarkson, S.-U. Alam, and D. J. Richardson, "High Gain Holmium-doped Fibre Amplifiers," *Optics Express* 24, 13946-13956 (2016).
- [18] N. Simakov, Z. Li, U. Alam, P. C. Shardlow, J. M. O. Daniel, D. Jain, J. K. Sahu, A. Hemming, W.A. Clarkson, and D. Richardson, "Holmium Doped Fiber Amplifier for Optical Communications at 2.05 – 2.13 μm ," in *Proc. OFC 2015*, Paper Tu2C.6.
- [19] A. Hemming, N. Simakov, M. Oermann, A. Carter, and J. Haub, "Record Efficiency of a Holmium-doped Silica Fibre Laser," in *Proc. CLEO 2016*, Paper SM3Q.5.
- [20] N. Simakov, A. Hemming, W. A. Clarkson, J. Haub, and A. Carter, "A cladding-pumped, tunable holmium doped fiber laser", *Optics Express* 21, 28415–28422 (2013).
- [21] N. Simakov, "Development of components and fibres for the power scaling of pulsed holmium-doped fibre sources," Ph.D. thesis (University of Southampton, 2017).
- [22] J. Wang, D. I. Yeom, N. Simakov, A. Hemming, A. Carter, S. B. Lee, and K. Lee, "Numerical modeling of in-band pumped Ho-doped silica fiber lasers," *J. Lightwave Technol.* 36, 5863–5880 (2018).
- [23] D. M. Baney, P. Gallion, and R. S. Tucker, "Theory and Measurement Techniques for the Noise Figure of Optical Amplifiers," *Optical Fiber Technology* 6, 122-154 (2000).